Available online at www.sciencedirect.com

ScienceDirect

Physica A 376 (2007) 173–190

PHYSICA A

www.elsevier.com/locate/physa

Binary modulated signal detection in a bistable receiver with stochastic resonance

Fabing Duan[a,*], Derek Abbott[b]

[a]Institute of Complexity Science, Qingdao University, Qingdao 266071, PR China
[b]Centre for Biomedical Engineering (CBME) and School of Electrical & Electronic Engineering, The University of Adelaide, Adelaide, SA 5005, Australia

Received 13 May 2006; received in revised form 1 October 2006
Available online 9 November 2006

Abstract

The archetypal bistable system can act as a nonlinear receiver for detecting binary signals modulated by amplitude, frequency, or phase. The introduction of noise enhances signal detection for a certain range of noise intensity, which is ascribed to non-conventional stochastic resonance (SR) phenomena, such as residual aperiodic SR and short-time SR. For the first time, we unify binary modulated signal detection from the point of view of an approximate probability density model. We develop both theoretical and numerical analyses of the receiver performance for each type of modulated signal. The optimization of receiver parameters and comparisons of the optimal bistable receiver versus the linear matched filter are also investigated. An interesting result is that the probability density model enables us to explore the SR range of noise intensity and the optimally-tuned bistable receiver theoretically, which may play a prominent role for nonlinear systems performing in noisy conditions.

Keywords: Bistable receiver; Residual aperiodic stochastic resonance; Short-time stochastic resonance; Receiver response speed; Signal detection

1. Introduction

A bistable system is the most frequently used model for characterizing stochastic resonance (SR) phenomena in diverse scientific fields [1–7]. In such systems, it is well known that, via the SR effect, the addition of noise can lead to an enhancement of the system response to weak signals. Moreover, experimental verification of SR effects has been demonstrated for a bistable characteristic, such as in a Schmitt trigger [8], bistable ring laser [9], paramagnetically driven bistable buckling ribbon [10], bistable electron paramagnetic resonance systems [11], bistable superconducting quantum interference devices [12], vertical cavity surface emitting lasers [13,14], bistable nanomechanical silicon oscillators [15,16]. In its early days, the SR phenomenon was strongly tied to the existence of a periodic weak subthreshold input—this is a keying feature of the conventional SR. Later, this effect was extended to aperiodic (i.e., broadband) input signals, leading to

*Corresponding author.
E-mail address: fabing1974@yahoo.com.cn (F. Duan).

0378-4371/$ - see front matter © 2006 Elsevier B.V. All rights reserved.
doi:10.1016/j.physa.2006.10.046

the term: aperiodic stochastic resonance (ASR) [17–21]. The relevance of ASR to the bistable system has attracted considerable attention in recent years [13,22–29]. A pioneering study on ASR considered this system for the transmission of a binary input sequence of fixed length [20]. Godivier and Chapeau-Blondeau [22] demonstrated that this system can be operated as a memoryless symmetric binary channel. Moreover, the information gain of optical bistable experimental systems has significantly shown SR [13,25], and this is beneficial to applications, such as optical communication and image processing [24]. Duan et al. studied the residual ASR effect in a bistable system driven by a suprathreshold random binary signal [28]. Recently, a new effect, named short-time SR, was explored in this nonlinear system for detecting frequency-shift keyed signals [29], which is consistent with a ring of coupled bistable systems operating as a short-term memory device in the SR regimes [23]. Interestingly, the demonstration of SR in a doubly clamped mechanical nanometre beam enables the exploration of SR in a quantum–mechanical context, which is at the very forefront of quantum logic and quantum computation [15,16]. These significant results clearly demonstrate the potential applicability of the bistable system in the signal processing field.

In the present paper, we investigate bistable receiver response to binary modulated signals, versus the amount of noise. Three kinds of binary modulated signals, representing the input information by their amplitudes, frequencies, or phases, are applied to this nonlinear receiver for exploiting its non-monotonic evolution with noise intensity. Besides the standard ASR effect, other non-conventional SR phenomena are observed and serve as detection mechanisms for various random binary modulated signals. An approximate but useful non-stationary probability density model is proposed to describe the mentioned non-conventional SR phenomena. Furthermore, we show that the optimal noise intensity in the SR regime can be theoretically evaluated in advance, which is useful for bistable systems adaptively harnessing low-level background noise. The optimally-tuned bistable receiver, for a fixed noisy binary signal, is also investigated and compared to the linear matched filter. This nonlinear receiver, that we shall consider in the following sections, can be viewed as an extension and generalization of these bistable systems, which may be of interest for electronic or optical bistable devices operating in a noisy environment. Therefore, the positive results will stimulate the latent applicability of the bistable system in a range of signal processing problems [15,28,29].

2. Binary modulated signal detection in a bistable receiver

In the transmission of digital information, an input information-bearing sequence $\{I\}$ is usually mapped onto a set of corresponding signal waveforms $S_m(t)$. In a symbol interval of T, these waveforms may differ in either amplitude or phase or frequency:

$$S_m(t) = \begin{cases} A_m, \\ A\cos(2\pi ft + \phi_m), \\ A\cos(2\pi f_m t), \end{cases} \tag{1}$$

for $(n-1)T \leqslant t \leqslant nT$, $n = 1, 2, \ldots$, and $m = 1, 2, \ldots, M$. Here, A_m, ϕ_m and f_m denote the set of M possible amplitudes, phases and carrier frequencies, corresponding to $M = 2^k$ possible k-bit symbols, respectively. In the following, we only focus on binary modulated signals with $M = 2$. Here, T is then called the bit interval. The input signals are (i) baseband binary pulse amplitude modulated (BPAM), (ii) binary phase-shift keyed (BPSK), and (iii) binary frequency-shift keyed (BFSK) signals. Note that the amplitude A and the carrier frequency f are fixed for BPSK signals, and have the same as the amplitude A for BFSK signals. Assume that the input symbols occur with equiprobabilities $P(S_1) = P(S_2) = \frac{1}{2}$ and have equal energy $\varepsilon = \int_0^T S_m^2(t)\,\mathrm{d}t$ $(m = 1, 2)$. The background noise $\eta(t)$ is zero-mean additive Gaussian white noise, with autocorrelation $\langle \eta(t)\eta(0) \rangle = 2D\delta(t)$ and the noise intensity D. Thus, the input signal-to-noise (SNR) ratio per bit, defined as $\varepsilon/4D$, is appropriate for measuring these noisy binary modulated input signals.

Next, the binary signals $S_m(t)$ plus the noise $\eta(t)$ arrive at a bistable dynamic receiver given as

$$\tau_a \frac{\mathrm{d}x(t)}{\mathrm{d}t} = x(t) - \frac{x^3(t)}{X_b^2} + S_m(t) + \eta(t), \tag{2}$$

with real receiver parameters τ_a and X_b [22,28]. This assumes a symmetrical double-well potential $V_0(x) = -x^2/2 + x^4/(4X_b^2)$, having two minima $V_0(\pm X_b) = -X_b^2/4$. In the absence of the noise $\eta(t)$, the minimal value of the amplitude A that destroys bistability in Eq. (2) occurs when $x - x^3/X_b^2 + A = 0$ ceases to have three real roots, and yields $A = 2X_b/\sqrt{27} \approx 0.38X_b$ [5,22]. For $A < 0.38X_b$, the input $S_m(t)$ alone is too small to induce transitions in the output $x(t)$, thus is referred to as subthreshold signal otherwise as suprathreshold signal [5,22,29].

In this paper, the signal detection statistics of the bistable receiver are measured by the total probability of detection error P_{er}

$$P_{\text{er}} = P(S_1)P(S_2|S_1) + P(S_2)P(S_1|S_2), \tag{3}$$

where $P(S_n|S_m)$ $(n, m = 1, 2,\ n \neq m)$ is the probability of error for the detected output to be $S_n(t)$, when the input signal is $S_m(t)$.

3. Probability density model and the total probability of detection error P_{er}

The total probability of detection error P_{er} can be deduced from an approximation of the non-stationary probability density of Eq. (2). The temporal relaxation of the non-stationary probability density, termed the receiver response speed λ_1, allows us to explicitly have a deeper understanding of the binary modulated signal detection in a nonlinear bistable receiver.

In each bit duration T, the system of Eq. (2) is subjected to the constant amplitude A_1 or $-A_1$ $(A_2 = -A_1)$ for BPAM signals, as shown in Fig. 1(a). On the contrary, the BFSK or BPSK signal has a ranges of amplitudes. Here, we take it as the first harmonic component of a rectangular signal waveforms with the same

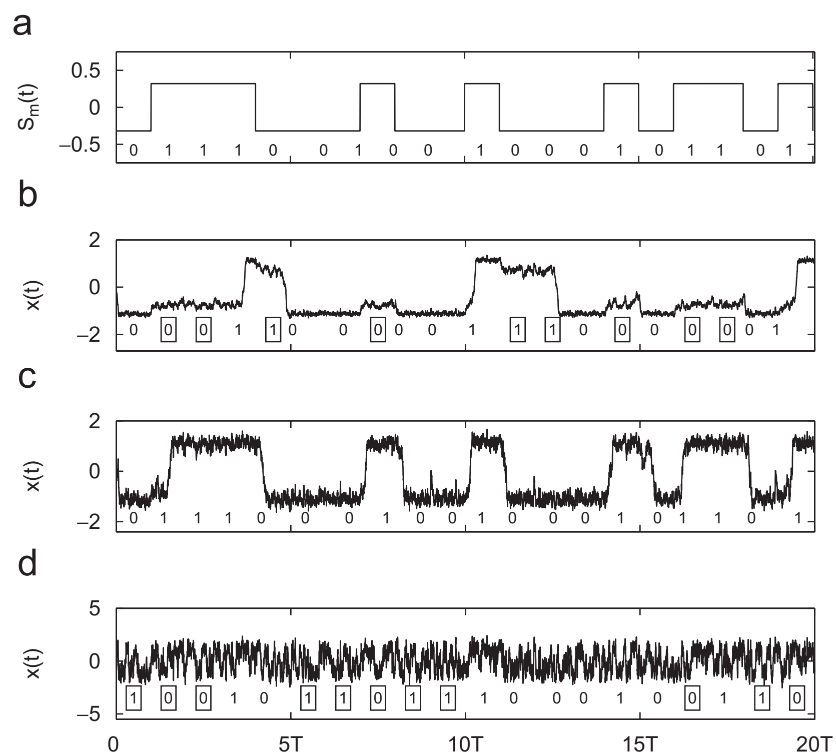

Fig. 1. Time evolution of baseband BPAM signal in the bistable receiver with $X_b = 1$ V and $\tau_a = 0.1$ s: (a) the baseband BPAM signal is with amplitude randomly taken from the set of {+0.32 V, −0.32 V} in each symbol interval of $T = 4$ s, representing the digits 0 and 1; the receiver output signal $x(t)$ at (b) the low level of noise ($D = 0.001\,\text{V}^2/\text{Hz}$, i.e., the input SNR per bit 20.1 dB), (c) the optimal noise intensity ($D = 0.008\,\text{V}^2/\text{Hz}$, i.e., 11.1 dB) and (d) the high noise level ($D = 0.1024\,\text{V}^2/\text{Hz}$, i.e., 0 dB). The decoded digits are given in the inset in terms of the decision threshold $\ell = 0$ V. The erroneous digits are boxed and the sampling time is $\Delta t = 10^{-3}$ s.

period f and the amplitude $\pi A/4$, as shown in Figs. 4(b) and 8(b). Note that a rectangular signal with amplitude $\pi A/4$ can be expressed as a series of harmonically related sinusoids $A\sum_{\mathrm{n=odd}} \sin(2n\pi ft)/n$. This simplification, although approximate, makes the model more amenable to theoretical analysis. However, it is emphasized that sinusoidal signals are retained in our simulations, wherein we numerically integrate Eq. (2) with the Euler–Maruyama discretization method and a small sampling time $\Delta t \ll \tau_a$ [22,28,30].

Now, in a short time interval, viz. each bit interval of T for BPAM signals or a half period for BFSK and BPSK signals, the system of Eq. (2) is subjected to a constant amplitude $S_m(t) = \pm A_s$. Here, A_s represents the corresponding amplitude of BPAM signals ($\pm A_1$), BFSK or BPSK signals ($\pm\pi A/4$). In the presence of noise $\eta(t)$, the statistically equivalent description for the corresponding probability density $\rho(x,t)$ is governed by the Fokker–Planck equation

$$\tau_a \frac{\partial\rho(x,t)}{\partial t} = \left[\frac{\partial}{\partial x} V'(x) + \frac{D}{\tau_a}\frac{\partial^2}{\partial x^2}\right]\rho(x,t), \tag{4}$$

where $V'(x) = -(x - x^3/X_b^2 \pm A_s)$. Here, $\rho(x,t)$ obeys natural boundary conditions such that it vanishes at large x for any t [31]. The steady-state solution of Eq. (4), for a constant input at $\pm A_s$, is given by

$$\rho(x|\pm A_s) = \lim_{t\to\infty} \rho(x,t) = C\exp\left[-\frac{\tau_a V(x)}{D}\right], \tag{5}$$

where C is a normalization constant [31]. As the amplitude varies from $\pm A_s$ to $\mp A_s$, we encounter the non-stationary solution $\rho(x,t)$ of the Fokker–Planck equation, i.e., Eq. (4). Here, we adopt the variational method [31] and obtain the eigenfunctions $u_i(x)$ corresponding to the eigenvalue λ_i for $i = 0, 1, \ldots, n$ [28]. The integer n is not increased in the iterative process until the preceding eigenvalues λ_i approximate the next ones within a tolerated error. Hence, $\rho(x,t)$ can be expanded, according to eigenfunctions and eigenvalues, as

$$\rho(x,t) = \sum_{i=0}^{n} C_i u_i(x) \exp\left[-\frac{\tau_a V(x)}{2D}\right] \exp[-\lambda_i t], \tag{6}$$

where C_i are normalization constants deduced from the orthogonal condition of eigenfunctions [31]. This analysis has been extensively deduced [28,29]. As for this variational method, the numerical results of the eigenvalues are very effective for determining the lowest eigenvalues [31]. Specifically, the inverse of the minimal positive eigenvalue, λ_1, is a measure of the slowest time taken by the bistable receiver to tend to the steady-state solution of Eq. (5). In other words, λ_1 is the speed of the bistable receiver tracing the variety of input signals, whence our term: receiver response speed. We here consider the non-stationary solution $\rho(x,t)$ for an input transition from $S_m(t) = \mp A_s$ to $S_m(t) = \pm A_s$, approximated with the two first terms from its asymptotic representation of Eq. (6), as

$$\rho(x,t) \simeq \rho(x|\pm A_s) + [\rho(x|\mp A_s) - \rho(x|\pm A_s)]\exp(-\lambda_1 t), \tag{7}$$

where $\rho(x|\pm A_s)$ are the steady-state solutions of Eq. (5) [28]. In Eq. (7), when $t = 0$, the term $\exp(-\lambda_1 t) = 1$ and $\rho(x,t)$ starts with the initial condition of $\rho(x|\mp A_s)$. As $t \to +\infty$, the term $\exp(-\lambda_1 t) = 0$, and $\rho(x,t)$ tends to the stationary condition of $\rho(x|\pm A_s)$. Therefore, this simple but generic probability density model of Eq. (7) is reasonable and applicable, as will be demonstrated in Section 4, for analyzing the detection of digitally modulated signals.

4. Theoretical and numerical studies on P_{er}

With the approximate non-stationary probability density model of Eq. (7), we will deduce theoretical expressions of total probability of detection error P_{er} for detecting the BPAM, BFSK and BPSK signals in this section. Also, numerical results will be presented for comparison. We find the detectability of the bistable receiver will behave as a non-monotonic function of the noise intensity—this is the signature of SR. Moreover, the appearance of SR effects, not restricted to the conventional SR, is extended for slightly suprathreshold amplitudes or in a short timescale of the bit interval, serving as a detection mechanism for binary modulated signal detection.

4.1. P_{er} for detecting baseband BPAM signals

It is well known that input source digits represented by baseband BPAM waveforms $S_m(t) = \pm A_1$ ($A_2 = -A_1$), as shown in Fig. 1, are emitted at a rate of one waveform every T and last over a duration T. In order to recover the successive input digits from the observation of the receiver output $x(t)$, we sample $x(t)$ at equispaced times $t_j = jT$ for $j = 1, 2, \ldots$. The sampled values $x_j = x(t_j)$ are compared to the decision threshold ℓ for decoding digits. In this communication process, we assume that the bit interval T, at which input digits are emitted, and the transition times at which one given pulse of duration T ends while the next pulse starts at the emitter, are both known at the receiver. This is a case of synchronized communication, as considered in Ref. [22]. The times t_j of the output readings are placed, as in Ref. [22], just at the end of one emitted pulse, just before the next pulse starts. This is to maximize the time allowed for $x(t)$ to approach the stable state, associated with the digit being currently transmitted.

In each symbol interval of T, the BPAM signal waveform takes an amplitude $-A_1$ or $+A_1$. Since the receiver output $x(t)$ is sampled at intervals jT for each decision, the term t in the probability density model of Eq. (7) should be replaced by T. Thus, the non-stationary probability density $\rho(x, T)$, at the times $t_j = jT$ for the transition from $S_m(t) = \mp A_1$ to $S_m(t) = \pm A_1$, or conversely, can be easily written as

$$\rho(x, T) \approx \rho(x| \pm A_1) + [\rho(x| \mp A_1) - \rho(x| \pm A_1)] \exp(-\lambda_1 T), \tag{8}$$

where $\rho(x| \pm A_1)$ are the steady-state solutions given in Eq. (5). Note that $\rho(x, T)$ are symmetrical for signal amplitudes $\pm A_1$, enabling us to address the performance of the nonlinear receiver.

Based on the maximum-likelihood criterion, the decision threshold ℓ can be calculated from

$$\rho(\ell, T| + A_1) = \rho(\ell, T| - A_1), \tag{9}$$

for decoding the information representing by input waveforms $S_m(t)$. Since the symmetric character of $\rho(x, T)$ for $S_m(t) = \pm A_1$, the decision threshold $\ell = 0\,\mathrm{V}$. Thus, the probability of error $P(S_n(t)|S_m(t))$ ($n, m = 1, 2$, $n \neq m$) can be expressed as

$$P(-A_1| + A_1) = \int_{-\infty}^{0} \rho(x, T| + A_1)\,\mathrm{d}x \tag{10}$$

and

$$P(+A_1| - A_1) = \int_{0}^{+\infty} \rho(x, T| - A_1)\,\mathrm{d}x. \tag{11}$$

Then, we can calculate the total probability of error P_{er} of Eq. (3) for detecting the baseband BPAM signals. Note that Eqs. (10) and (11) hold for signal waveforms $S_m(t)$ with equiprobability. Also, when Eqs. (10) and (11) are introduced in Eq. (3), it is apparent that the term $\exp(-\lambda_1 T)$ should satisfy the condition of $\exp(-\lambda_1 T) \leqslant \frac{1}{2}$, i.e., λ_1 should not be sufficiently small compared to T. It is in this case that P_{er} falls below $\frac{1}{2}$, and that effective binary transmission can take place [32]. The following quantitative results are all calculated in this regime where $\exp(-\lambda_1 T) \leqslant \frac{1}{2}$ [28].

Fig. 2 shows the numerical simulations and the theoretical results for the bistable receiver detecting baseband BPAM signals. The theoretical curves are plotted in Fig. 2(b) in terms of Eqs. (8)–(11). In comparison to the numerical data of Fig. 2(a), this probability density model can describe the receiver's performance in the SR region well. Furthermore, Fig. 2(c) compares theoretical and numerical results for three given signal amplitudes. It is emphasized that the discrepancy between the theoretical and realized values of simulations can be attributed to several factors. One being, in Eq. (8), the receiver response speed only considers the lowest, i.e., λ_1. Moreover, we assume that the receiver firstly reaches the stable state associated to $\mp A_1$ at $(j-1)T$, then evolves into the state corresponding to $\pm A_1$ at jT, as shown in Eq. (8). However, it does not hold if the state of $\mp A_1$ at $(j-1)T$ is not stable. This non-stationary case is difficult to consider comprehensively. Nevertheless, this theory captures the essential features of standard ASR behavior, in this kind of nonlinear receiver, for detecting subthreshold BPAM signals, viz. $A_1 < 0.38 X_b$.

In line with residual SR [33], we also identified a new ASR phenomenon, i.e., residual ASR, to survive in a single bistable dynamic system subject to a fast suprathreshold random BPAM signal [28]. Generally, standard

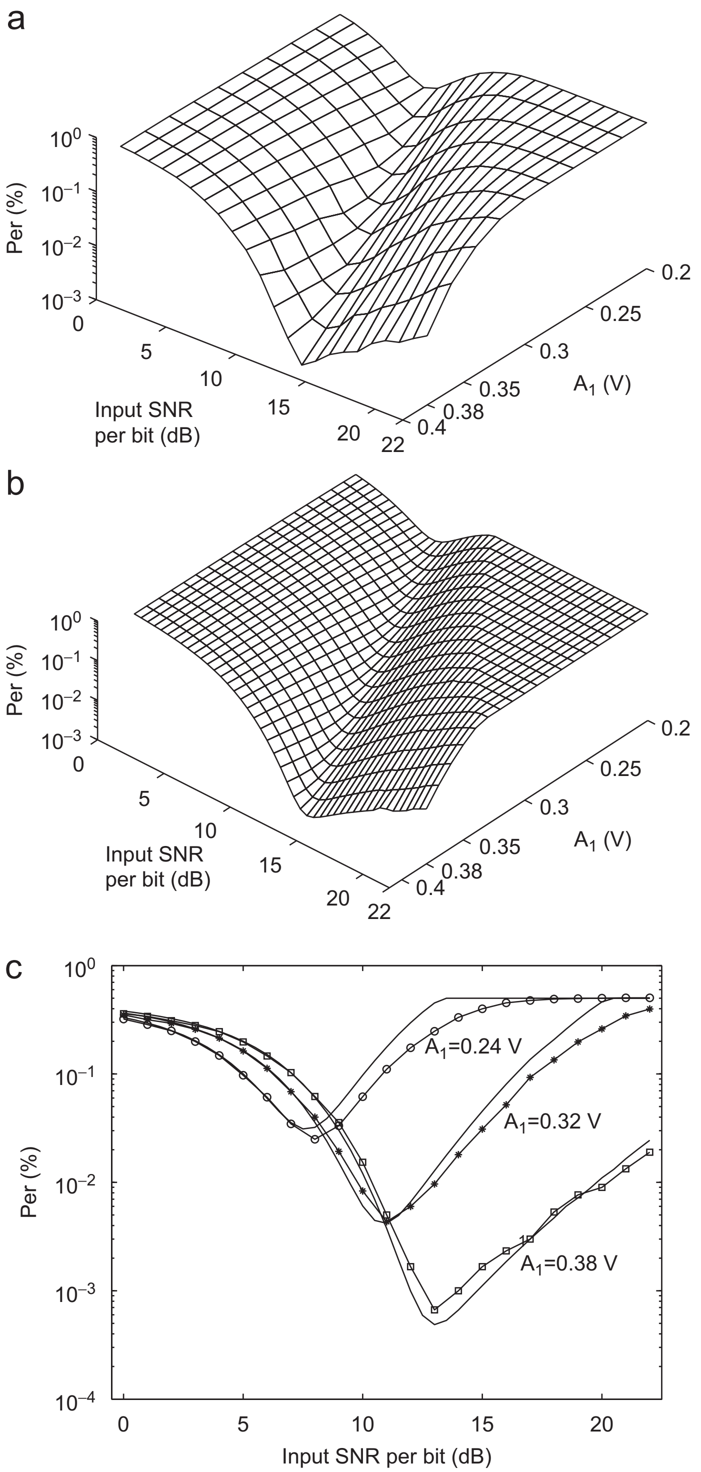

Fig. 2. Numerical (a) and theoretical (b) results for P_{er} versus the input SNR per bit and the signal amplitude A_1 for detecting baseband BPAM signals. The bistable receiver parameters are $X_b = 1\,V$ and $\tau_a = 0.1\,s$. Here, the bit interval $T = 4\,s$ and the sampling time is $\Delta t = 10^{-3}\,s$. (c) The idiographic comparisons of numerical data with theoretical results of P_{er} for $A_1 = 0.24\,V$ (circles), $A_1 = 0.32\,V$ (stars) and $A_1 = 0.38\,V$ (squares).

ASR (subthreshold) [17] is more like an amplitude effect, wherein a small aperiodic input has an amplitude too small to trigger transition at the output, and it gets assistance from noise for that. In contrast to standard ASR, residual ASR (suprathreshold) is a temporal effect, wherein a slow dynamic system has difficulty to follow the variations imposed by a fast (suprathreshold) input, and it receives spurred by the noise for that. By this mechanism, as demonstrated in Ref. [28], information detection from a fast suprathreshold input can be enhanced by addition of noise. However, the input signal has to remain a little suprathreshold, but not too much, otherwise the positive effect of noise tends to vanish, whence our term "residual." We have studied the detection of suprathreshold baseband BPAM signals via the residual ASR effect, in more detail in Ref. [28]. Particularly, the theoretical probability density model of Eq. (8) is also valid for the slightly suprathreshold input, as $A_1 > 0.38X_b$, as shown in Fig. 3, wherein the response of the dynamic bistable receiver is relatively slower for fast suprathreshold BPAM signals. Hence, input noise plays a constructive role in improving the receiver's performance via the residual ASR effects.

4.2. P_{er} for detecting BFSK signals

In our previous work of Ref. [29], we established the possibility of decoding subthreshold or slightly suprathreshold M-ary FSK signals in bistable receivers, via a series of short-time SR phenomena. Usually, conventional SR is characterized with a statistical measurement, e.g. the output SNR, resulting from long-term observational data [3,5]. In contrast, we are more interested in the noise-enhanced effects that occur in each short-term duration of each bit interval as the noise intensity increases—what we called the short-time SR phenomenon [29]. Here, short-time SR is emphasized as being in a short-term timescale of the bit interval, whereas we are in a standard situation of ASR for a long-term data statistics. Since the ASR phenomenon cannot cover all features of the detection of M-ary FSK signals, short-time SR is claimed in regard to the adaptive ability of a bistable receiver to timescale and frequency variations [29]. Due to the transient nature of the input waveform in each bit interval, we decode the digital information with a rule based on zero crossing times, rather than a statistical measurement. In this paper, the bytes represented by the corresponding input BFSK signals with frequency f_m are decoded as

$$(f_{m-1} + f_m)T \leqslant N_m < (f_m + f_{m+1})T, \tag{12}$$

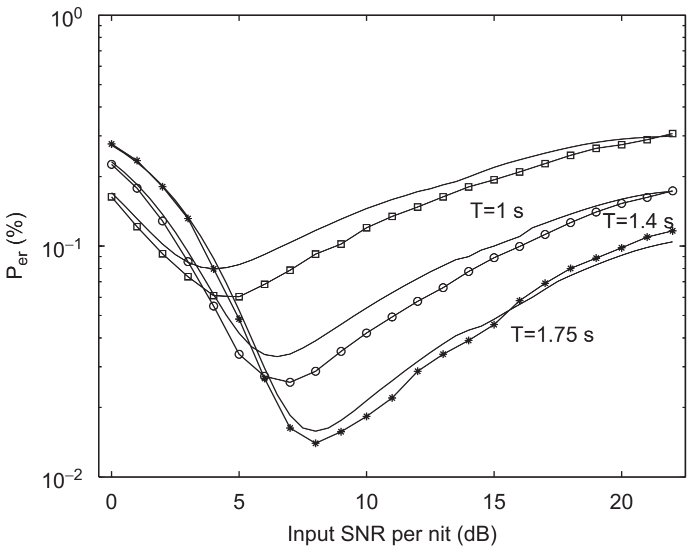

Fig. 3. The comparison of numerical data with theoretical results of P_{er} for $A_1 = 0.4$ V at $T = 1$ s (squares), $T = 1.4$ s (circles), $T = 1.75$ s (stars). The input signals are suprathreshold as $A_1 > 0.38X_b$, while the bit intervals T are fast by comparing with the system switching time of 1.76 s, as introduced in Ref. [28]. Other parameters are same as in Fig. 2.

with the frequency separation $\Delta f = f_{m+1} - f_m$ for $m = 1, 2, \ldots, M$ and $\Delta f = 1/(2T)$ represents the minimum frequency separation between adjacent signals for orthogonality of the M-ary FSK signals. Then, the output information sequence can be decoded. Particularly, we only consider the performance of bistable receivers for detecting BFSK signals ($M = 2$) in this paper. By comparing input and decoded sequences, the measure of total probability of detection error P_{er} of Eq. (3) is obtained to quantify the performance of this nonlinear receiver.

For simplicity, we transform the input sinusoidal waveforms $S_m(t) = A\cos(2\pi f_m t)$ in each bit interval T into a square wave, as shown in Fig. 4(b), with the same frequency f_m and the equivalent amplitude $A_s = \pi A/4$. This is deduced from the fact that a rectangular signal can be expressed as a series of harmonically related sinusoids, as stated previously. In each bit interval of T, we sample the bistable receiver output $x(t)$ with the sampling frequency of $f_s > 2\max(f_m)$ ($m = 1, 2$) for counting the zero crossing times N_m. Fig. 5 shows an example of the receiver output $x(t)$ for the BFSK signal $S_m(t) = 0.5\cos(12\pi t)$ in one bit interval $T = 1$ s. The discrete samples x_j are also inserted at each sampling time $j/f_s = j/20$ s for $j = 1, 2, \ldots$. The zero crossing times, N_m, depend on the signs of discrete samples x_j. As the equivalent square waveforms exchange the amplitudes $\pm\pi A/4$ each half period of $1/(2f_m)$, the correct probabilities of signs at samples x_j can be theoretically calculated as

$$P_c^{x_j} = \begin{cases} \int_0^{+\infty} \rho(x, t'_{p_j})\,\mathrm{d}x & \text{if } p_j = +A_s, \\ \int_{-\infty}^{0} \rho(x, t'_{p_j})\,\mathrm{d}x & \text{if } p_j = -A_s, \end{cases} \tag{13}$$

where t'_{p_j} are the time differences between the sampling times j/f_s and the anterior zero crossing times t_n ($n = 1, 2, \ldots$). For example, $t'_{p_{11}}$, as shown in Fig. 5 (a), is the sampling time $11/f_s$ minus the anterior zero crossing time t_6. The non-stationary probability density $\rho(x, t'_{p_j})$ takes the relevant expression from Eq. (7) in terms of $p_j = +A_s$ or $p_j = -A_s$; this is Eq. (13). Here, p_j are the sampling values in equivalent square waves, as plotted in Fig. 5(a).

In the presence of noise, the zero crossing times N_m counted by the sign sequence of samples x_j will be in the vicinity of $2f_m T$ even in the SR region of noise, as shown in Fig. 4(c). If N_m enters into the region, determined by the decision rule of Eq. (12), the digit carried by the BFSK signals will be correctly decoded at receiver.

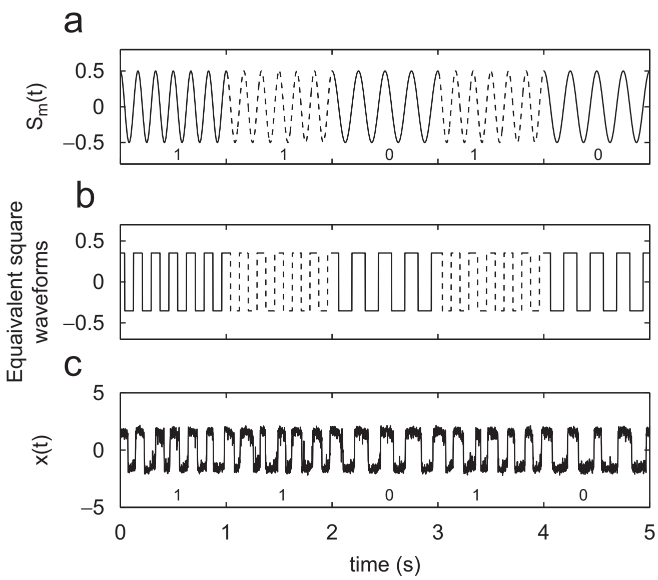

Fig. 4. (a) The BFSK signal $S_m(t) = 0.5\cos(2\pi f_m t)$ with carrier frequencies 4 or 6 Hz randomly in each bit interval of $T = 1$ s, representing binary digits 0 or 1, respectively. (b) The equivalent transformed square waveforms with same frequencies and the amplitude $A_s = \pi A/4 = \pi/8$ V in each bit interval. (c) The receiver output signal $x(t)$ for the BFSK signal $S_m(t)$. Here, $X_b = 1.5$ V, $\tau_a = 10^{-3}$ s and $D = 1.97 \times 10^{-4}\,\mathrm{V}^2/\mathrm{Hz}$, i.e., the input SNR per bit 22.1 dB. The sampling time $\Delta t = 10^{-4}$ s and the decoded binary digits are also inserted.

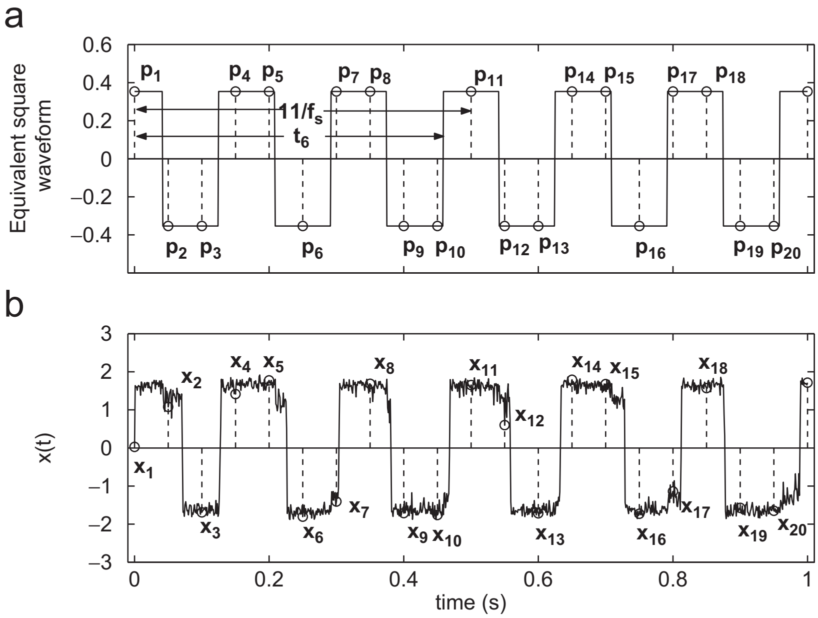

Fig. 5. (a) The equivalent square waveforms with same frequencies 6 Hz for the BFSK signal $S_m(t) = 0.5\cos(12\pi t)$ in one bit interval of $T = 1$ s. The discrete samples p_j are illustrated at each sampling time $j/f_s = j/20$ s for $j = 0, 1, 2, \ldots, f_sT$. (b) The receiver output $x(t)$ for the BFSK signal $S_m(t)$. The discrete samples x_j are also inserted at each sampling time $j/f_s = j/20$ s . Other parameters are same as in Fig. 4.

Moreover, N_m can be theoretically calculated by the joint probability $\prod_{i=1}^{f_sT} P_c^{x_j}$ in each bit interval of T with the statistical independence assumption. However, such zero crossing times N_m obtained by the sign combinations of x_j are too large to be totally counted. Alternatively, we can decode the digits as zero crossing times N_m just equals to $2f_mT$. The aim is to compare the above theoretical analysis with the corresponding numerical results, as illustrated in Fig. 6(b) and (c).

In this process, it is found that the phase shift of $x(t)$ induced by the nonlinearity of receivers in each half period, or the dynamical inter-well transition, frequently results in erroneous signs of the samples x_j just as $x(t)$ crosses the zero level. For example, the samples x_2, x_7, x_{12} and x_{17} presented in Fig. 5(b) have erroneous signs relative to the input amplitudes of p_2, p_7, p_{12} and p_{17}. Fortunately, if the noise intensity is in the SR region, and there are two samples in each half period, these erroneous signs of the samples x_j do not change the zero crossing times $N_m = 2f_mT$ as $f_s > 2\max(f_m)$. Nevertheless, we must retain the single sample in one half period or a potential well. Thus, the correct probability of detecting $S_m(t)$ is the joint correct probability of $P_c^{x_j}$ excluding these samples x_j that just follow $x(t)$ crossing the zero level and make no contributions to zero crossing times. Then, the error probability of detecting information, digits 1 or 0, is one minus the corresponding correct probability. Finally, the total probability of error P_{er} for detecting $S_m(t)$ is then obtained for the theoretical formula of Eq. (3). Fortunately, this complicated analysis is not cumbersome, since the BFSK signal only has two difference modulated frequency f_m for $m = 1, 2$.

Although our discussion of the probability of error P_{er} is somewhat abbreviated, and the discrepancy between theoretical and numerical calculations exists, as shown in Figs. 6 and 7, this theoretical analysis does provide us with some important insights into the BFSK signal detection in nonlinear receivers. For example, it can elicit the optimal noise intensity region for the further research in adaptive signal processing, in this nonlinear system, as addressed in the section below. It is also interesting to note that even if the modulated signal amplitude $A > 0.38X_b$ is slightly suprathreshold for the receiver, the total probability of detection error P_{er} also evolves a non-monotonic behavior as the noise intensity D increases, as seen in Fig. 7. This can be attributed to the residual SR effects in a short timescale of T (more detailed discussion is in Refs. [29,33]). In addition, we have investigated the behavior of the bistable receiver when the phase shift is not known or random. It was observed that the detectability of the bistable receiver is almost same for different phase shifts

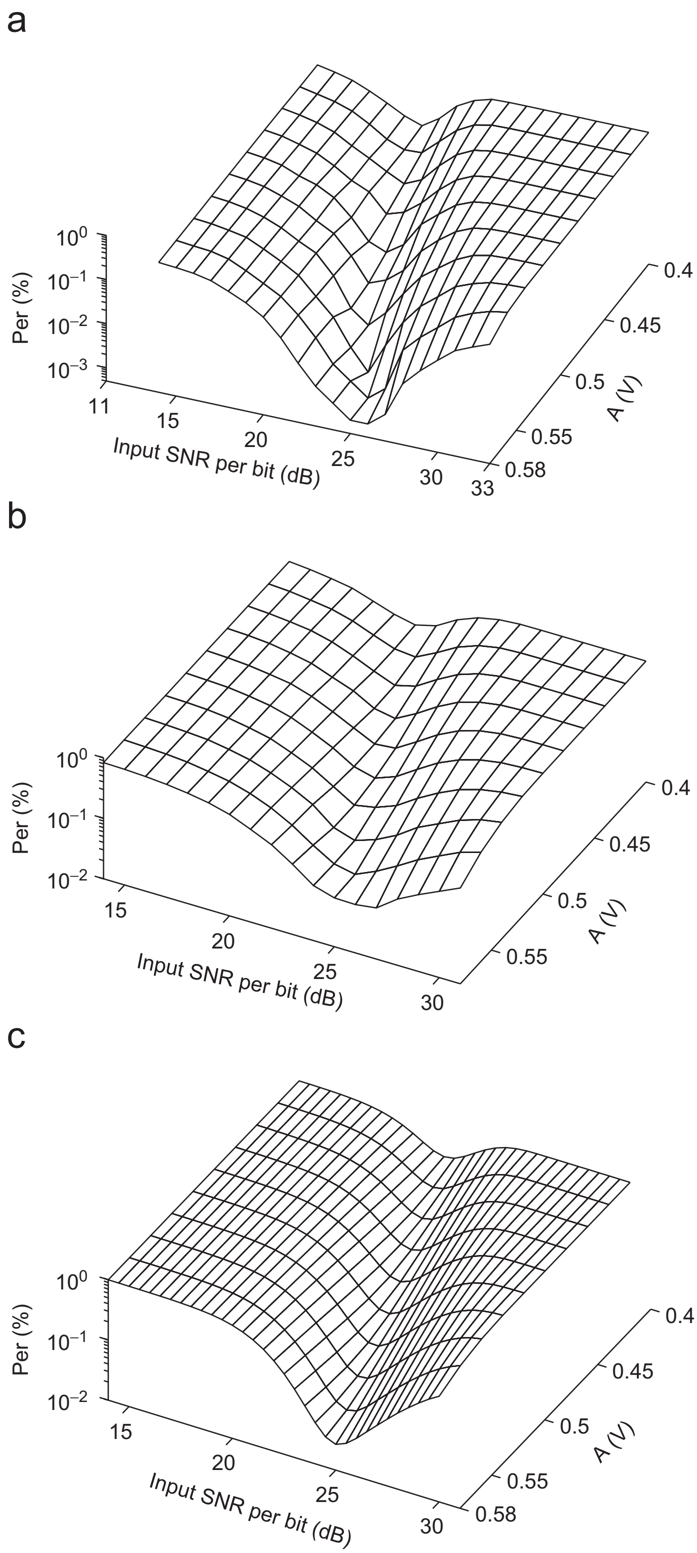

Fig. 6. Numerical results of P_{er} as a function of the signal amplitude A and the noise density D for (a) the decoding scheme $(f_{m-1}+f_m)T \leqslant N_m < (f_m+f_{m+1})T$, viz. Eq. (12), and (b) the simple decision rule of $N_m = 2f_mT$. (c) The theoretical results of P_{er} as a function of A and D for the reduced decision rule $N_m = 2f_mT$. Here, $T = 1\,\mathrm{s}$ and $\Delta t = 10^{-4}\,\mathrm{s}$. The receiver parameters are $X_b = 1.5\,\mathrm{V}$ and $\tau_a = 10^{-3}\,\mathrm{s}$.

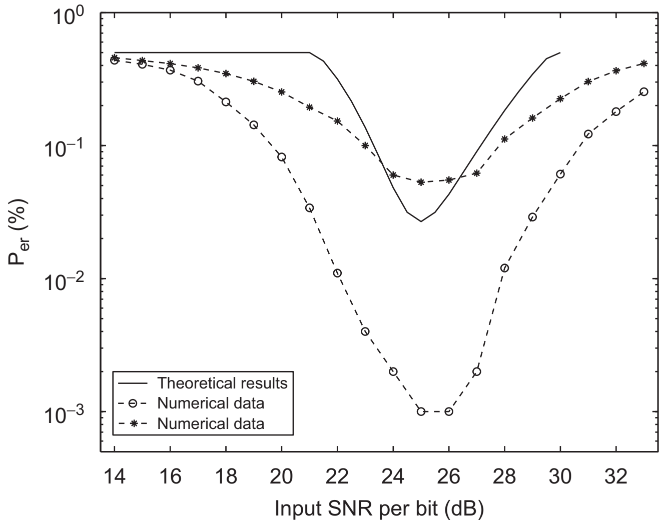

Fig. 7. A specific view of P_{er} as a function of D for $A = 0.58\,\text{V}$. The dashed lines are numerical data for the reduced decision rule $N_m = 2f_mT$ (stars) and the decoding scheme $(f_{m-1} + f_m)T \leqslant N_m < (f_m + f_{m+1})T$ (circles). The solid line is theoretical results. Other parameters are same as in Fig. 6.

for deciphering M-ary FSK signals [29]. Unknown or random phase shift seems not to affect this detection strategy, whereas the zero crossing times are decided as $(f_{m-1} + f_m)T \leqslant N_m < (f_m + f_{m+1})T$. This indicates that the bistable receiver is robust to the phase shift and applicable when the carrier phase is unknown at the receiver and estimation of its values remains an open question [29].

4.3. P_{er} for detecting BPSK signals

In this subsection, the BPSK signals are considered as $S_m = A\cos(2\pi ft + 2(m-1)\pi/M)$, with $1 \leqslant m \leqslant M$, $0 \leqslant t \leqslant T$, the carrier frequency f and $M = 2$. Then, the information, digits 0 and 1, are represented by the signal phases $\phi_1 = 0$ and $\phi_1 = \pi$, or conversely. At the output of nonlinear receivers, we are also interested in the short data record of each bit interval of T. Consequently, the short-time SR mechanism also plays a key role in detecting the BPSK signals at the receiver outputs, as in aforementioned BFSK signal detection. However, the decision rule is simpler than that of decoding the BFSK signal. Fig. 8 shows an example of the BPSK modulated signals and the receiver output $x(t)$. It is seen that the receiver follows the input signal synchronously to some extent, by the assistance of noise. Since the BPSK signal has two antipodal waveforms of $S_1(t)$ and $S_2(t)$, the decision rule can be simply adopted as deciding signs of sample values $x_j = x(jT)$ at jT for $j = 1, 2, \ldots,$ that is, the positive sign of x_j for $\phi_1 = 0$ (digits 0) and the negative one of x_j for $\phi_2 = \pi$ (digits 1).

The approximate theory of total error probability for detecting the BPSK signals can also resort to the equivalent square waveforms with the same frequency f and the amplitude $A_s = \pi A/4$ in each bit interval. The error probabilities of $P(S_n(t)|S_m(t))$ $(n, m = 1, 2,\ n \neq m)$ can be approximately calculated using Eqs. (10) and (11). Noting that the term of T in the right side of Eqs. (10) and (11) should be replaced with $1/(4f)$, as well as the equivalent signal amplitude A_s instead of A. A detailed comparison of numerical and theoretical data of P_{er} is illustrated in Fig. 9. The results demonstrate that the bistable receiver detects the BPSK signals with a resonance-like behavior as the noise intensity varies. However, an examination of Fig. 9(c) suggests that although the theoretical analysis presents P_{er} as the right quantity, it shifts the resonance curve to a higher region of the input SNR per bit, i.e., the lower noise intensity, on the whole. Hence, the approximate probability density model cannot perfectly describe the detection performance of a bistable receiver for BPSK signals. The distinction also comes down to our simple assumptions in the above theoretical development.

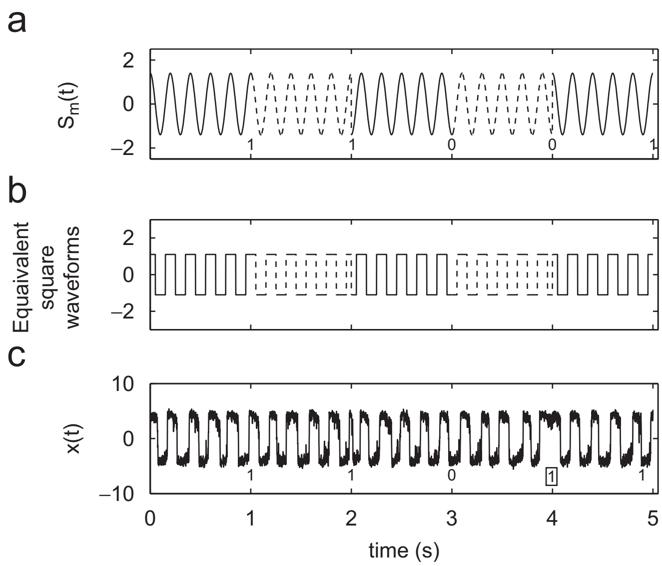

Fig. 8. (a) An example of the BPSK signal $S_m(t) = 1.4\cos(10\pi t + \phi_m)$ with $\phi_1 = 0$ and $\phi_2 = \pi$. The corresponding binary digits are also inserted; (b) the equivalent square waveforms with the same frequency and the amplitude $A_s = \pi A/4$; (c) the receiver output $x(t)$ at $D = 3 \times 10^{-4}\,\mathrm{V^2/Hz}$. Here, $X_b = 3.8\,\mathrm{V}$, $\tau_a = 10^{-3}\,\mathrm{s}$, $T = 1\,\mathrm{s}$ and $\Delta t = 10^{-4}\,\mathrm{s}$.

In this subsection, our treatment of the demodulation of BPSK signals assumes that the receiver has a perfect estimate of the phase shift induced by the channel including the receiver itself. Consequently, a delayed sampling time will be adjusted more or less in numerical simulations for decoding the information sampling values, by ignoring the phase shift induced by this nonlinear channel [32].

5. The optimal SR values of noise intensity

In practical applications, it is meaningful for nonlinear systems to find the best performance at an optimal noise level in noisy circumstances. Using the theoretical results from the above sections, we might predict the optimal noise intensities D_{optimal} for the detection of the BPAM, BFSK and BPSK signals, this is, minimizing P_{er} for a fixed input signal and a given receiver. Although the total probability of error P_{er} is a unimodal function of D, as shown in Figs. 2, 6 and 9, D_{optimal} is hard to analytically derive from the partial derivative of P_{er} to the noise intensity D. The reason is that the term $\exp(-\lambda_1 t)$ of Eq. (7) is a variational function of D. In this paper, we determine the D_{optimal} by an iterative computation as the contiguous values satisfy a sufficient tolerated error. Fig. 10 shows that the theories developed in the above sections agree with the numerical optimal noise intensities of the BPAM and the BFSK signals well, while they fail to estimate that of the BPSK signals. Furthermore, it is noted that the optimal input SNR, per bit (in decibel), is more like a linear function of the input signal amplitude. This suggests a simple adaptation principle for the nonlinear receivers to properly improve their operating level, via adding noise.

Until now, we have focus on the behavior of P_{er} as a functions of the noise intensity D. In terms of the principle of tuning noise intensity, a nonlinear system can improve its detectability by adding more noise if the initial given noise level is lower than the optimal value. However, this tuning method will encounter the difficult case of the worse noise intensity lying beyond the optimal regime for a single system. Given a fixed noise intensity, we have discussed the approach of tuning system parameters for realizing SR effects in Refs. [27,35]. Fortunately, this generic probability density model of Eq. (7) is also applicable for the corresponding theoretical framework. The systems with parameter $X_b < \sqrt{27}A/2$ are more efficient in the view of information detection, but at the risk of not employing the positive role of noise. The conclusion presented in Refs. [27,35] argues that SR, with adaptively controlled noise intensity, may be of interest for a

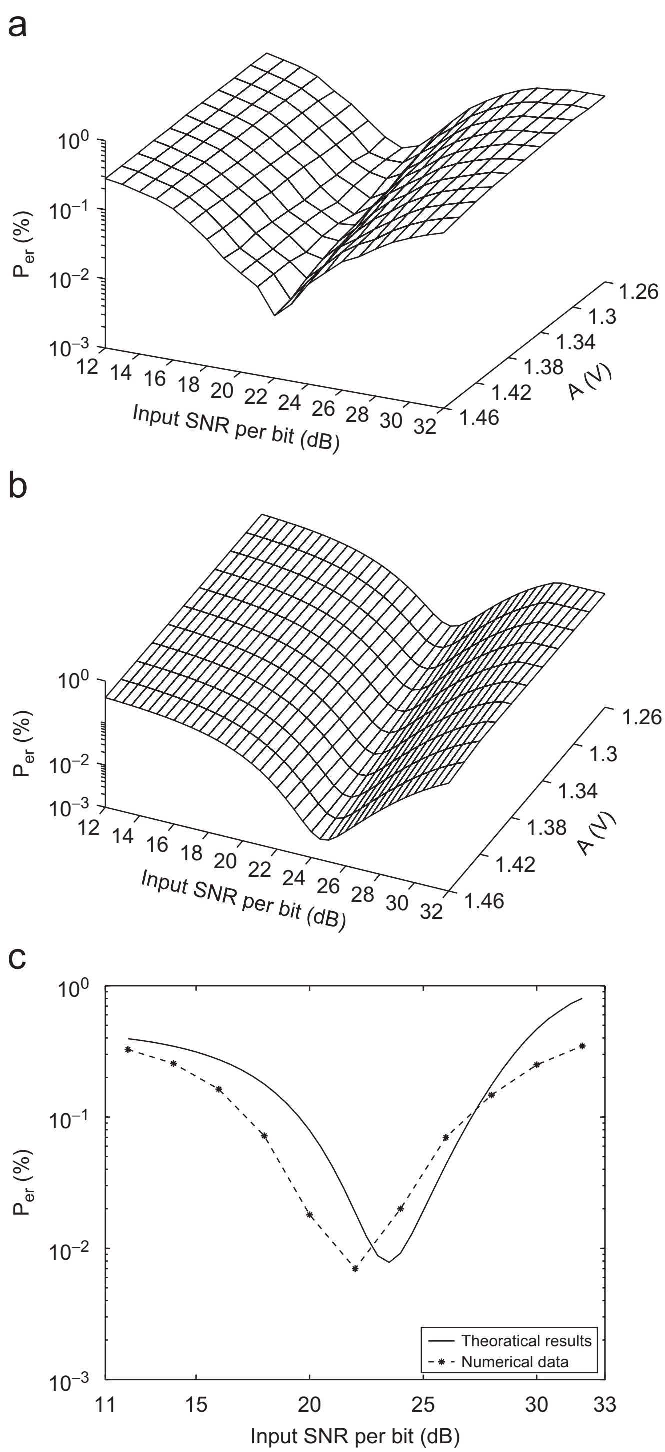

Fig. 9. Numerical (a) and theoretical (b) results of P_{er} as a function of the signal amplitude A and the noise density D for the BPSK signal $S_m(t) = A\cos(10\pi t + \phi_m)$. (c) Plots of P_{er} as a function of the noise density D for $A = 1.46\,\mathrm{V}$. Other parameters are same as Fig. 8.

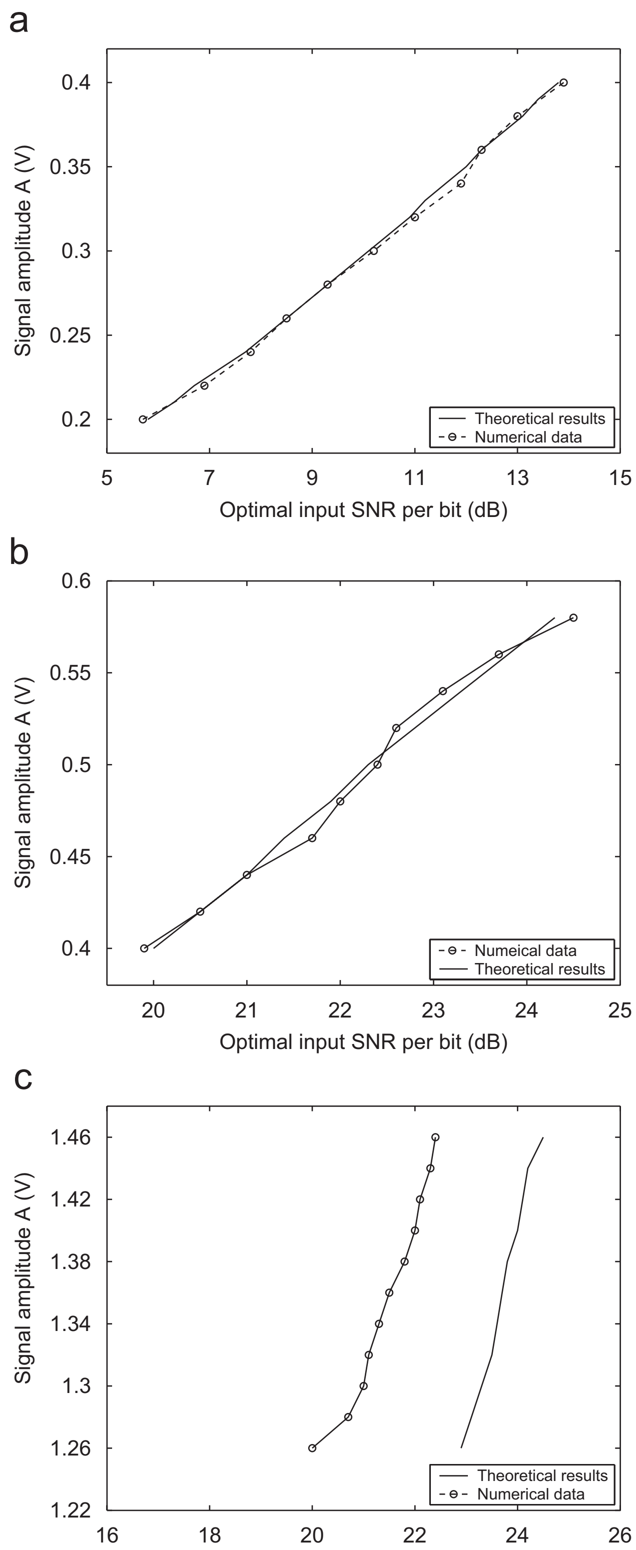

Fig. 10. The optimal input SNR per bit versus the input signal amplitude of (a) the BPAM, (b) the BFSK and (c) the BPSK signals. The corresponding receiver parameters, input signals and numerical simulation preferences are same as in Figs. 2, 6 and 9, respectively. The optimal input SNR per bit is obtained for the minimum P_{er} numerically (dashed lines) and theoretically (solid lines).

non-adjustable nonlinear systems, working in relatively low-noise environments. The present study still indicates a meaningful way of enhancing the performance of nonlinear systems without controllable parameters. It is also worthy of noting that even if the worse noise intensity is beyond the optimal regime for a single system, an uncoupled parallel array of threshold systems can improve its performance via SR effects [36]. This largely extends the applicability of SR to a widely signal processing scope.

6. Tune receiver parameters and comparison of the optimally-tuned bistable receiver versus the linear matched filter

In above sections, we adopted three bistable systems to complete different tasks of random binary modulated signal detection, of which receiver parameters are not designedly selected. If we assume that the nonlinear bistable system is adjustable, it is interesting to tune the receiver parameters (X_b, τ_a) to constitute an optimal receiver with the lowest P_{er} at a fixed input SNR per bit.

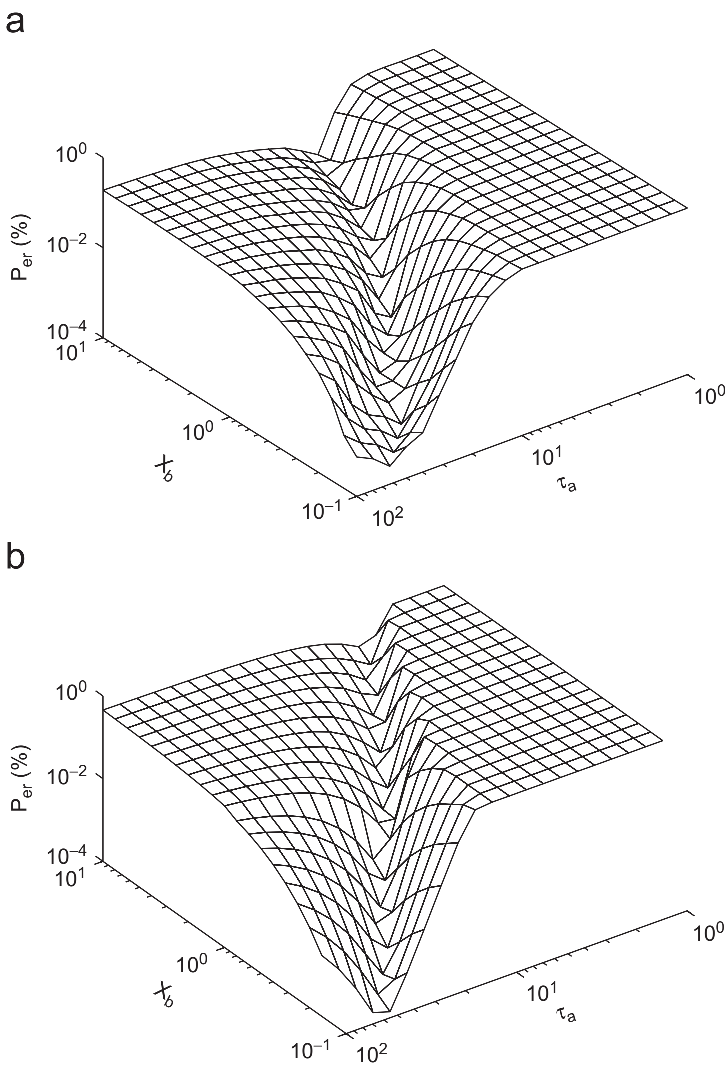

Fig. 11. Numerical (a) and theoretical (b) results of P_{er} as a function of receiver parameters (X_b, τ_a) for the BPAM signal detection. Here, $A = 0.32\,\mathrm{V}$, $T = 4\,\mathrm{s}$ and $\Delta t = 0.01\tau_a$, and $D = 0.008\,\mathrm{V}^2/\mathrm{Hz}$.

An example of P_{er} is illustrated in Fig. 11 for the BPAM signal detection. The numerical result of P_{er}, as shown in Fig. 11(a), agrees well with the theoretical data in Fig. 11(b). The parameters (X_b, τ_a), corresponding to the bottom points of P_{er}, represent optimal choices of nonlinear receiver of Eq. (2). For a given noisy input, the methodology of tuning system parameters is as follows: Choose the parameter X_b the smallest as possible, and then deduce the optimal corresponding parameter τ_a such that P_{er} is minimal, at the risk of operating outside the region where SR appears [27,35]. Moreover, the optimal pair of parameters (X_b, τ_a) is not exclusive. These conclusions have been explained in detail in Refs. [27,35]. It is noted that the theoretical probability density model of Eq. (8) is feasible to predicate the optimal parameters (X_b, τ_a), as shown in Fig. 11(b).

It is interesting to compare bistable receiver to matched filter for detecting binary modulated signals [27,37]. The matched filter is a linear optimal filter achieving the overall minimal P_{er} [32]. Here, we focus on the BPAM signal detection. Given conditions in Fig. 11, the theoretical total probability of error of the matched filter is $P_{\mathrm{er}} = 2.1 \times 10^{-7}$, while an optimal bistable receiver, for example, the receiver with parameters ($X_b = 10^{-1}$, $\tau_a = 10^{1.8}$) presents $P_{\mathrm{er}} = 3 \times 10^{-4}$. Similar results are also given in Refs. [27,37]. It is seen that the matched filter is, expectedly, always better than the bistable receiver. However, as much as the noise intensity D increases, the performance of the optimal bistable receiver becomes close to that of the matched filter. Interestingly, the optimal bistable receiver can outperform the matched filter in the presence of desynchronization between the decision time and the end of each pulse on BPAM signals [27]. Thus, the bistable receiver belongs to a kind of robust nonlinear filter in varying conditions, such as the desynchronization [27] and the detection of signals with unknown parameters [37]. In this paper, we assume that the interval T at which input digits are emitted, and the transition times at which one given pulse of duration T ends while the next pulse starts at the emitter, are both known at the receiver. This is a case of synchronized communication, as considered in Ref. [32]. We also note that the effect of inter-symbol-interference on the observed behavior of the bistable receiver is investigated in Ref. [38]. A more reasonable probability density model is theoretically deduced [38]. In the present paper, the bistable receiver shows its multifold abilities in detecting three kinds of binary modulated signals. These significant results verify the potential applicability of the bistable system in signal detection field.

7. Conclusion

In summary, we have explored the detectability of the bistable receiver, in terms of the total error probability measure, for detecting the BPAM, BFSK and BPSK signals. An approximate, but generic, probability density model is theoretically investigated for each kind of digitally modulated signal. The total error probability of the bistable receiver can be derived from this uniform probability density model, by comparing it with the numerical simulation results in detail. It was demonstrated that the phenomenon of SR acts as an enhancing mechanism for detecting digitally modulated signals, and different forms exist, such as the residual ASR and the short-time SR effects. These are non-conventional SR phenomena in contrast to the conventional SR phenomenon of detecting the subthreshold periodic inputs over a long observed time. Furthermore, we develop a methodology to predict the optimal noise intensity for the bistable receiver at its optimal performance, i.e., the minimum total error probability. The corresponding theoretical analyses show that the probability density model performs well for estimating the optimal noise intensity for the BPAM and BFSK signals, but fails for the BPSK signals. Furthermore, this study indicates that the optimal input SNR per bit is more like that of a linear function of the input amplitude, numerically and theoretically. This suggests a simple adaptive methodology for operating bistable systems in noisy circumstances, by adding an appropriate amount of noise to the input. Finally, the optimization of receiver parameters and comparisons of the optimal bistable receiver versus the linear matched filter are investigated. The present study, incorporating the previous research on the robust and the computational saving of the bistable systems [27–29,35,37], verifies the good performance of nonlinear systems in broad conditions.

Acknowledgments

We gratefully thank the anonymous reviewers for their constructive comments and suggestions. This work is sponsored by NSFC (No. 60602040), "Taishan Scholar" PSP, the SRF for ROCS, SEM and PhD

PFME of China (No. 20051065002). Funding from the Australian Research Council (ARC) is gratefully acknowledged.

References

[1] R. Benzi, A. Sutera, A. Vulpiani, The mechanism of stochastic resonance, J. Phys. A 14 (1981) L453–L458.
[2] B. McNamara, K. Wiesenfeld, Theory of stochastic resonance, Phys. Rev. A 39 (1989) 4854–4869.
[3] L. Gammaitoni, P. Hänggi, P. Jung, F. Marchesoni, Stochastic resonance, Rev. Mod. Phys. 70 (1998) 233–287.
[4] K. Wiesenfeld, F. Moss, Stochastic resonance and the benefits of noise: from ice ages to crayfish and SQUIDs, Nature 373 (1995) 33–36.
[5] F. Moss, D. Pierson, D. O'Gorman, Stochastic resonance: tutorial and update, Int. J. Bifurcation Chaos 4 (1994) 1383–1397.
[6] A.R. Bulsara, L. Gammaitoni, Tuning in to noise, Phys. Today 49 (1996) 39–45.
[7] A. Allison, D. Abbott, Stochastic resonance on a Brownian ratchet, Fluctuation Noise Lett. 1 (2002) L239–L244.
[8] S. Fauve, F. Heslot, Stochastic resonance in a bistable system, Phys. Lett. A 97 (1983) 5–8.
[9] B. McNamara, K. Wiesenfeld, R. Roy, Observation of stochastic resonance in a ring laser, Phys. Rev. Lett. 60 (1988) 2626–2629.
[10] M.L. Spano, M. Wun-Fogle, W.L. Ditto, Experimental observation of stochastic resonance in a magnetoelastic ribbon, Phys. Rev. A 46 (1992) 5253–5256.
[11] L. Gammaitoni, M. Martinelli, L. Pardi, S. Santucci, Phase shift in bistable EPR systems at stochastic resonance, Phys. Lett. A 158 (1991) 449–452.
[12] A. Hibbs, E. Jacobs, J. Bekkedahl, A. Bulsara, F. Moss, Stochastic resonance in a bistable SQUID loop, in: P. Handel, A.L. Chung (Eds.), Noise in Physical Systems and $1/f$ Fluctuations, AIP Press, New York, 1993, pp. 720–723.
[13] S. Barbay, G. Giacomelli, F. Marin, Experimental evidence of binary aperiodic stochastic resonance, Phys. Rev. Lett. 85 (2000) 4652–4655;
S. Barbay, G. Giacomelli, F. Marin, Stochastic resonance in vertical cavity surface emitting lasers, Phys. Rev. E 61 (2000) 157–166.
[14] J. Houlihan, D. Goulding, Th. Busch, C. Masoller, G. Huyet, Experimental investigation of a bistable system in the presence of noise and delay, Phys. Rev. Lett. 92 (2004) 050601.
[15] R.L. Badzey, P. Mohanty, Coherent signal amplification in bistable nanomechanical oscillators by stochastic resonance, Nature 437 (2005) 995–998.
[16] A.R. Bulsara, No-nuisance noise, Nature 437 (2005) 962–963.
[17] J.J. Collins, C.C. Chow, T.T. Imhoff, Aperiodic stochastic resonance in excitable systems, Phys. Rev. E 52 (1995) R3321–R3324.
[18] F. Chapeau-Blondeau, Noise-enhanced capacity via stochastic resonance in an asymmetric binary channel, Phys. Rev. E 55 (1997) 2016–2019.
[19] G.P. Harmer, B.R. Davis, D. Abbott, A review of stochastic resonance: circuits and measurement, IEEE Trans. Instrum. Meas. 51 (2002) 299–309.
[20] G. Hu, D. Gong, X. Wen, C. Yang, G. Qin, R. Li, Stochastic resonance in a nonlinear system driven by an aperiodic force, Phys. Rev. A 46 (1992) 3250–3254.
[21] M.D. McDonnell, N.G. Stocks, C.E.M. Pearce, D. Abbott, Stochastic resonance and data processing inequality, Electron. Lett. 39 (2003) 1287–1288.
[22] X. Godivier, F. Chapeau-Blondeau, Stochastic resonance in the information capacity of a nonlinear dynamic systems, Int. J. Bifurcation Chaos 8 (1998) 581–589.
[23] M.F. Carusela, R.P.I. Perazzo, L. Romanelli, Stochastic resonant memory storage device, Phys. Rev. E 64 (2001) 031101.
[24] M. Misono, T. Kohmoto, Y. Fukuda, M. Kunitomo, Noise-enhanced transmission of information in a bistable system, Phys. Rev. E 58 (1998) 5602–5607.
[25] M. Misono, T. Kohmoto, M. Kunitomo, Y. Fukuda, Information gain in an optical bistable system by stochastic resonance, Phys. Rev. E 67 (2003) 061102.
[26] A.R. Bulsara, C. Seberino, L. Gammaitoni, Signal detection via residence-time asymmetry in noisy bistable devices, Phys. Rev. E 67 (2003) 016120.
[27] D. Rousseau, J. Rojas-Verela, F. Duan, F. Chapeau-Blondeau, Evaluation of a nonlinear bistable filter for binary signal detection, Int. J. Bifurcation Chaos 15 (2005) 667–679.
[28] F. Duan, D. Rousseau, F. Chapeau-Blondeau, Residual aperiodic stochastic resonance in a bistable dynamic system transmitting a suprathreshold binary signal, Phys. Rev. E 69 (2004) 011109.
[29] F. Duan, D. Abbott, Signal detection for frequency shift keying via short time stochastic resonance, Phys. Lett. A 344 (2005) 401–410.
[30] T.C. Gard, Introduction to Stochastic Differential Equations, Marcel Dekker Inc., New York, 1998.
[31] H. Risken, The Fokker–Planck Equation: Methods of Solution and Applications, Springer Series in Synergetics, second ed., Springer, Berlin, 1989.
[32] J.G. Proakis, Digital Communications, third ed., McGraw-Hill, New York, 1995.
[33] F. Apostolico, L. Gammaitoni, F. Marcheson, S. Santucci, Resonant trapping: a failure mechanism in switch transitions, Phys. Rev. E 55 (1997) 36–39.

[35] B. Xu, F. Duan, F. Chapeau-Blondeau, Comparison of aperiodic stochastic resonance in a bistable system by adding noise and tuning system parameters, Phys. Rev. E 69 (2004) 061110.
[36] F. Chapeau-Blondeau, D. Rousseau, Enhancement by noise in parallel arrays of sensors with power-law characteristics, Phys. Rev. E 70 (2004) 060101 (R).
[37] F. Duan, D. Abbott, Q. Gao, Evaluation of bistable systems versus matched filters in detecting bipolar pulse signals, Fluctuation Noise Lett. 5 (2005) L127–L142.
[38] J. Li, X. Pan, A nonlinear monostable filter for bipolar pulse signal detection, Mech. Systems Signal Process. (2006), in press.